Eur. Phys. J. E **3**, 259–271 (2000)

THE EUROPEAN PHYSICAL JOURNAL E

EDP Sciences

Adhesion-induced lateral phase separation in membranes

S. Komura[1,2,a,b] and D. Andelman[2]

[1] Department of Materials and Interfaces, Weizmann Institute of Science, Rehovot 76100, Israel
[2] School of Physics and Astronomy, Raymond and Beverly Sackler Faculty of Exact Sciences, Tel Aviv University, Ramat Aviv 69978, Tel Aviv, Israel

Received 12 January 2000 and Received in final form 15 May 2000

Abstract. Adhesion between membranes is studied using a phenomenological model, where the inter-membrane distance is coupled to the concentration of sticker molecules on the membranes. The model applies to both adhesion of two flexible membranes and to adhesion of one flexible membrane onto a second membrane supported on a solid substrate. We mainly consider the case where the sticker molecules form bridges and adhere directly to both membranes. The calculated mean-field phase diagrams show an upward shift of the transition temperature indicating that the lateral phase separation in the membrane is *enhanced* due to the coupling effect. Hence the possibility of adhesion-induced lateral phase separation is predicted. For a particular choice of the parameters, the model exhibits a tricritical behavior. We also discuss the non-monotonous shape of the inter-membrane distance occurring when the lateral phase separation takes place. The inter-membrane distance relaxes to the bulk values with two symmetric overshoots. Adhesion mediated by other types of stickers is also considered.

PACS. 87.16.-b Subcellular structure and processes – 68.10.-m Fluid surfaces and fluid-fluid interfaces – 82.70.-y Disperse systems

1 Introduction

Adhesion of membranes and vesicles has attracted considerable experimental and theoretical interest because of its prime importance to many bio-cellular processes [1,2]. Theoretical treatments of membranes composed of single component lipid bilayers have revealed that generic interactions such as van der Waals, electrostatic or hydration interactions govern the adhesive properties of interacting membranes. It is also worthwhile to mention that related phenomena are found in unbinding transition of nearly flat membranes [3] or adhesion of vesicles to surfaces [4].

In addition to general non-specific interactions mentioned above, it is known from the works of Bell and coworkers [5,6] as well as others [7], that highly specific molecular interactions play an essential role in biological adhesion. This interaction acts between complementary pairs of proteins such as ligand and receptor, or antibody and antigen. A well-studied example of such coupled systems is the biotin-avidin complex. The avidin molecule has four biotin binding sites, two on each side, and forms a five-molecule biotin-avidin-biotin complex. The resulting specific interaction is highly local and short-ranged. Measurements by surface force apparatus [8] or atomic force microscopy [9,10] have shown that the force required to break a biotin-avidin bond is about 170 pN. In related experiments measuring chemical equilibrium constants [11], it was found that the biotin-avidin binding energy is about 30–35 $k_{\mathrm{B}}T$ which is larger than thermal fluctuations. Other coupled systems are those of selectins and their sugar ligands where the bond is much weaker, of the order of $5k_{\mathrm{B}}T$ [12,13].

More recently several models taking into account thermal fluctuations in membrane adhesion have been proposed. Zuckerman and Bruinsma [12,13] used a statistical mechanics model which is mapped onto a two-dimensional Coulomb plasma with attractive interactions. They predicted an enhancement of the membrane adhesion due to thermal fluctuations. In another work, Lipowsky considered the adhesion of lipid membranes which includes anchored stickers, *i.e.*, anchored molecules with adhesive segments [14,15]. It was shown that flexible membranes can adhere if the sticker concentration exceeds a certain threshold. If the multi-component membranes, including lipids and sticker molecules, undergo a phase separation, the adhesion is dominated by the sticker-rich domains. Further studies in this direction using mean-field theory and Monte Carlo simulations [16] obtained a phase separation which is driven both by attractive intra-membrane sticker interactions and fluctuation-induced interactions between stickers.

[a] On leave from Faculty of Computer Science and Systems Engineering, Kyushu Institute of Technology, Iizuka 820-8502, Japan.
[b] *Present address*: Department of Chemistry, Tokyo Metropolitan University, Tokyo 192-0397, Japan.

The problem of multi-component membrane adhesion is intimately related to that of formation of domains (a lateral phase separation). This has been observed by several experiments. For example, the biotin-avidin interaction occurring during vesicle-vesicle adhesion was investigated by a micropipette technique [17]. The adhesion between one avidin-coated vesicle and a second biotinylated vesicle is followed by an accumulation of biotin-avidin complex in the contact zone. This accumulation of cross-bridges between the two vesicles is found to be a diffusion-controlled process.

Adhesion-induced phase separation has been observed by Albersdörfer *et al.* and results from the interplay between long-range repulsive and short-range attractive interactions [18,19]. The membrane includes repeller molecules in the form of lipopolymers (modified DOPE lipid with a polyethyleneoxide headgroup), mimicking glycocalix in real biological systems. The other component is a receptor molecule in the form of biotinylated lipids (DOPE-X-biotin). This lipopolymer is responsible for longer-range repulsive interaction, while the short-range attractive interaction is introduced by adding streptavidin to the extra-cellular solution. The streptavidin acts as a connector between the biotinylated lipids on the two membranes. A technique of reflection interference contrast microscopy [20] was used to observe domain formation on a vesicle adhering to a membrane supported on a solid substrate. The lateral phase separation on both membranes leads to the formation of domains of tight adhesion separated by domains of loose adhesion [18,19].

In a related work, adhesion between cationic vesicles and anionic supported membranes revealed that electrostatic interactions induce lateral charge segregation on the membrane [21,22]. This phase separation leads to patches of tight inter-membrane contact and decoupled "blisters". Furthermore, adhesion of membranes including self-recognizing homophilic molecules and lipopolymers has been investigated [23]. It was found that the initial weak adhesion is followed by slower aggregation into tightly bound domains coexisting with domains of weak adhesion. The result has been interpreted in terms of a double-well inter-membrane interaction potential due to the presence of the lipopolymers. Let us emphasize that in all the above-mentioned experiments, it was reported that adhesion molecules aggregate spontaneously and form domains of tight adhesion.

It is generally believed that multi-component biomembranes in physiological conditions are close to their critical point, and membrane functions are partially governed through phase separation processes. Moreover, concentration fluctuations in the vicinity of the critical point may affect biophysical properties of membranes and can be of importance in regulating membrane processes in a robust way. Recently this conjecture was supported by an experiment of an insoluble Langmuir monolayer at the air/water interface [24,25]. The monolayer was prepared in two different steps. The first mimics the composition of the inner leaflet of a cell biomembrane, while the second mimics the outer leaflet. In both cases, by using fluorescence microscopy technique, it was found that the Langmuir monolayer is close to its corresponding critical point of demixing.

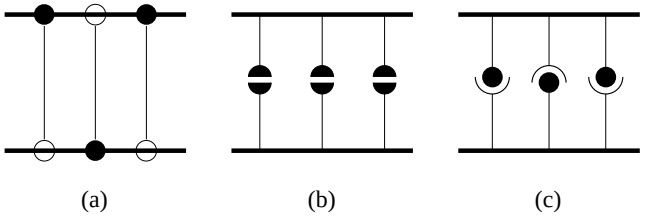

Fig. 1. Schematic representation of various types of adhesion between two membranes. The two membranes are represented by black lines. (a) Bolaform-sticker adhesion: bridges consist of a single type of sticker molecules which are anchored to one membrane (filled circle) and stick to the other membrane by another sticky part of the molecules (open circle). (b) Homophilic-sticker adhesion: bridges consist of two identical stickers which are bound together by their respective sticky end segments. (c) Lock-and-key adhesion: bridges consist of two different stickers forming a ligand-receptor type bond.

So far, the interplay between lateral phase separation and membrane adhesion has not been considered theoretically in detail except in references [14–16]. The work in references [21,22] deals only with the specific case of oppositely charged membranes. In this paper we provide a general phenomenological approach for the adhesion of multi-component membranes. Using a mean-field theory, we investigate how the lateral phase separation within the membrane is affected by the adhesion of membranes. Like in references [14–16], we consider adhesion mediated by sticker molecules. Sticker molecules are polymers or macromolecules anchored to one membrane and interacting with the other membrane by another sticky part of the molecule. They can form bridges between two adjacent membranes (so-called *trans*-interaction) [14], and play an essential role in the adhesion of cell membranes in biological systems.

We distinguish three types of adhesion depending on the structure of bridges as represented in Figure 1. i) "Bolaform-sticker" adhesion where each bridge molecule consists of a single sticker having two sticky ends (Fig. 1(a)). One sticker end is anchored to one membrane while the other end is adhering directly to the second membrane. ii) "Homophilic-sticker" adhesion where the bridges are formed by two stickers of the same type (Fig. 1(b)). Each sticker is anchored on one of the membranes, while their free ends bind together to form the bridge. iii) "Lock-and-key" adhesion where the bridges consist of two different stickers forming a ligand-receptor type bond (Fig. 1(c)). This case represents an asymmetric adhesion due to the lack of symmetry between the ligand and receptor. In the present work, we mainly discuss the symmetric bolaform-sticker adhesion (case i) above) using a model where the equilibrium spacing between two membranes is coupled to the local concentration of stickers. Even in the latter symmetric case, a certain asymmetry can be obtained by controlling separately the sticker chemical potentials on the

two membranes. An important consequence of our model is that the lateral phase separation is *enhanced*.

This paper is organized as follows. In the next section, we explain our phenomenological model of bolaform-sticker adhesion. The mean-field phase diagrams are given in Section 3. The inter-membrane distance between two coexisting domains is calculated in Section 4. Finally discussion is provided in Section 5 where the other types of adhesion mentioned above are considered.

2 Bolaform-sticker adhesion

In this section, we treat the case where the adhesion is mediated by a single type of sticker molecules which are anchored irreversibly to one membrane and stick to the other membrane by another sticky part of the molecules as in Figure 1(a). The anchor segments consist of a hydrophobic segment and penetrate into the hydrophobic interior of the lipid bilayer. The sticky segments, on the other hand, adhere directly to another membrane having some potential of sticking [15]. As mentioned above, we call this a "bolaform-sticker". Consider two interacting membranes labeled by $i = 1, 2$ consisting of lipid molecules and bolaform-stickers as schematically shown in Figure 2. Let the sticker concentration in each membrane be denoted by $\psi_i(\boldsymbol{r})$, where $\boldsymbol{r} = (x, y)$ is a two-dimensional planar vector and $0 \leq \psi_i(\boldsymbol{r}) \leq 1$. Note that the average concentrations of stickers on the two membranes, $\langle\psi_1\rangle$ and $\langle\psi_2\rangle$, do not have to be the same.

When the adhesion molecules are very flexible, they can bend back to form arches on a single membrane. In order to avoid such a situation in experiments and in the model, the bending rigidity of the sticker molecules should be sufficiently large. Hence we assume that for stiff enough stickers all the bonds are inter-membrane ones connecting the two separate membranes as considered in references [14,15].

The interaction between two stickers on the same membrane is called *cis*-interaction and can be repulsive or attractive. Here we discuss the case in which this interaction is attractive. Then, below a certain critical temperature, the multi-component membrane undergoes a first-order phase transition and stickers form lateral domains. As shown in Figure 3, a sticker-poor phase coexists with a sticker-rich phase in the two-phase region of the phase diagram. The sticker critical concentration ψ_c and the critical temperature T_c are assumed to be the same for the two planar membranes. We define the concentration difference $\phi_i(\boldsymbol{r})$ for each of the membranes with respect to the critical concentration by

$$\phi_i(\boldsymbol{r}) = \psi_i(\boldsymbol{r}) - \psi_c \qquad (i = 1, 2), \tag{2.1}$$

where ϕ_i satisfies $-1 \leq \phi_i \leq 1$.

The total free energy of the two coupled membranes can be written as a sum of several terms detailed below. The first contribution describes the lateral phase separation of each membrane. Motivated by recent experiments on Langmuir monolayers [24,25] demonstrating that the inner and outer leaflets of biomembranes are close to their critical point, we employ a phenomenological Ginzburg-Landau free energy which is an expansion in powers of the order parameters $\{\phi_i\}$. Hence we have

$$F_1 = \frac{1}{2}\sum_{i=1,2}\int \mathrm{d}^2\boldsymbol{r}\,\left[\frac{1}{2}c(\nabla\phi_i)^2 + \frac{1}{2}t\phi_i^2 + \frac{1}{4}\phi_i^4 - \mu_i\phi_i\right]. \tag{2.2}$$

This expansion for the free energy can be justified close to a critical point where the ϕ_i's are small enough. The parameter c representing the line tension acting at the domain boundary, and the reduced temperature

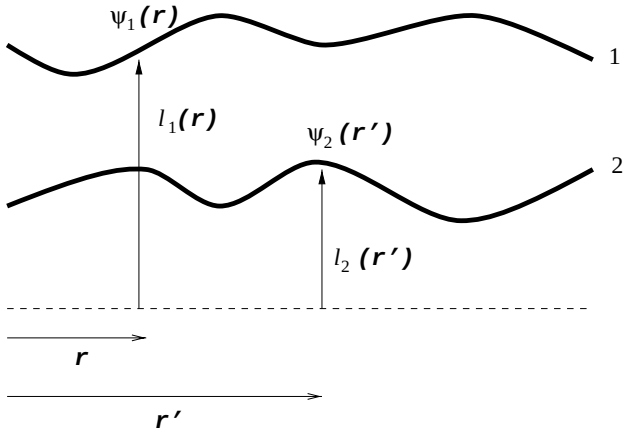

Fig. 2. Two adhering membranes. The reference x-y plane is shown as a dashed line. The height of two membranes measured from this plane is denoted as ℓ_1 and ℓ_2, respectively. The sticker concentration on each membrane is denoted by ψ_1 and ψ_2, respectively.

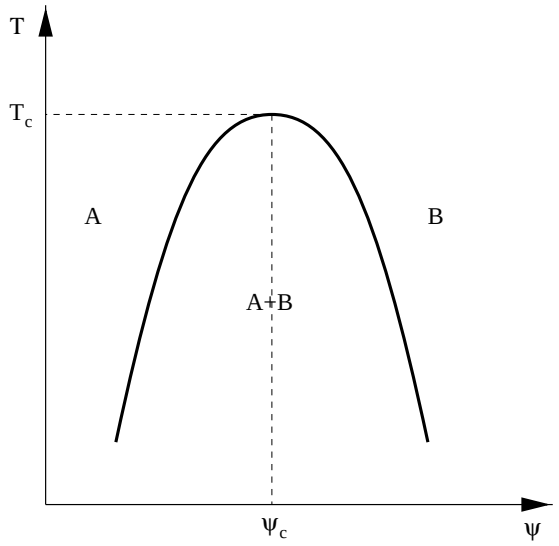

Fig. 3. Schematic phase diagram for a single membrane containing sticker molecules. The concentration of the sticker molecule is ψ. The critical concentration and the critical temperature is denoted by ψ_c and T_c, respectively. Within the coexistence curve the membrane separates into sticker-rich and sticker-poor region (A+B coexistence). The membrane is in a one-phase outside the coexistence curve.

$t = (T - T_c)/T_c$ are taken to be the same for the two membranes. On the other hand, the chemical potential μ_i, coupled to the membrane sticker concentration ϕ_i, can differ between the two membranes since the sticker concentrations on the two membranes do not have to be the same. We recall that each bolaform-sticker is modeled with one of its ends anchored irreversibly to one membrane, while the second sticky end is attracted by the second membrane. The sticker concentration is associated with the anchored end of the stickers. The normalization factor 1/2 in (2.2) is introduced in order to write down the free energy per single membrane. The coefficient of the fourth-order term can generally be set as a positive constant without loss of generality.

It is convenient to introduce the following new variables for the average and the difference between the two concentrations:

$$\phi_+ = \frac{\phi_2 + \phi_1}{2} = \frac{\psi_2 + \psi_1}{2} - \psi_c,$$
$$\phi_- = \frac{\phi_2 - \phi_1}{2} = \frac{\psi_2 - \psi_1}{2}, \tag{2.3}$$

where $-1 \le \phi_+ \le 1$ and $-1 \le \phi_- \le 1$. In terms of these new variables, (2.2) can be written as

$$F_1 = \int \mathrm{d}^2\boldsymbol{r} \left[\frac{1}{2}c\left[(\nabla\phi_+)^2 + (\nabla\phi_-)^2\right] + \frac{1}{2}t(\phi_+^2 + \phi_-^2) + \frac{1}{4}(\phi_+^4 + 6\phi_+^2\phi_-^2 + \phi_-^4) - \mu_+\phi_+ - \mu_-\phi_-\right], \tag{2.4}$$

where

$$\mu_+ = \frac{\mu_2 + \mu_1}{2}, \qquad \mu_- = \frac{\mu_2 - \mu_1}{2}. \tag{2.5}$$

The chemical potential μ_- associated with the order parameter ϕ_- is non-zero when the symmetry between the two membranes is explicitly broken. Namely, the two interacting membranes have different average concentrations of stickers.

Next we consider the out-of-plane deformation energy of the two membranes. As depicted in Figure 2, the membrane shape is parameterized by their heights $\ell_1(\boldsymbol{r})$, $\ell_2(\boldsymbol{r}')$, above the x-y reference plane. Working in the Monge representation it is implicitly assumed that the membranes remain flat on average and have no overhangs. This approach can be also useful to treat adhesion of vesicles in their contact zone. When the vesicle is large enough, it will be roughly flat close to the contact region, and the entire vesicle can be thought of as a reservoir for the stickers. Returning to the deformation energy, it can be written as the sum of the bending energy and the surface tension of each of the two membranes separately, as well as the interacting potential energy between them [26,27]:

$$F_2 = \frac{1}{2}\sum_{i=1,2}\int \mathrm{d}^2\boldsymbol{r}\left[\frac{1}{2}\kappa(\nabla^2\ell_i)^2 + \frac{1}{2}\sigma(\nabla\ell_i)^2\right] + \int \mathrm{d}^2\boldsymbol{r}\; v(\ell_1 - \ell_2; \psi_1, \psi_2), \tag{2.6}$$

where κ is the bending rigidity, σ is the mechanical surface tension acting on the membranes, and v is the potential energy per unit area representing the inter-membrane interactions. For simplicity, κ and σ are assumed to be equal for the two membranes and do not vary as a function of the sticker concentration ψ_i. The potential $v(\ell_1 - \ell_2; \psi_1, \psi_2)$ can be generally assumed to be a function of the local relative height coordinate $\ell_1 - \ell_2$ and the sticker concentration ψ_i. The former assumption is the so-called Derjaguin approximation [28]. The dependence on the sticker concentration ψ_i will be considered later.

We now make a change of variables and transform to the center of mass and relative coordinates given, respectively, by

$$L = \frac{\ell_2 + \ell_1}{2}, \qquad \ell = \frac{\ell_2 - \ell_1}{2}. \tag{2.7}$$

Only terms which depend on ℓ can be considered in the case where the center of mass is stationary, hence L is a constant of motion. Then (2.6) can be written as [30]

$$F_2 = \int \mathrm{d}^2\boldsymbol{r}\left[\frac{1}{2}\kappa(\nabla^2\ell)^2 + \frac{1}{2}\sigma(\nabla\ell)^2 + v(\ell; \psi_1, \psi_2)\right]. \tag{2.8}$$

In the high-temperature phase, the stickers are homogeneously distributed, and each of the membrane is in a one-phase region on the phase diagram. We assume that even in the absence of sticker molecules, such membranes are bound to each other due to the balance between the short-range repulsive (*e.g.*, hydration interaction) and longer-range attractive interactions (*e.g.*, van der Waals interaction). Hence, we do not consider the interesting problem of the unbinding transition [14–16]. Although the membranes are always bound together, their equilibrium distance ℓ depends on the sticker concentration. Let us consider the potential $v(\ell; \psi_1, \psi_2)$ in (2.8) for $\phi_+ = 0$. Note that $\phi_+ = 0$ means that $(\psi_1 + \psi_2)/2 = \psi_c$, namely, the average sticker concentration on the two membranes is at its critical value ψ_c. The inter-membrane potential $v(\ell; \phi_+ = 0)$ is assumed to have a single minimum at a certain inter-membrane distance $\ell = \ell_0$ for $\phi_+ = 0$. This gives the equilibrium distance between the two bound membranes. The deviation of the inter-membrane distance from ℓ_0 is defined by the dimensionless quantity $\delta(\boldsymbol{r})$ given by

$$\delta(\boldsymbol{r}) = \frac{\ell(\boldsymbol{r}) - \ell_0}{\ell_0}. \tag{2.9}$$

For small deviations from the minimum of the potential, $v(\ell; \phi_+ = 0)$ can be expanded to second order. This is known as the harmonic approximation and gives

$$v(\ell; \phi_+ = 0) \approx v(\ell_0) + \frac{1}{2}v''(\ell_0)(\ell - \ell_0)^2 = v(\ell_0) + \frac{1}{2}V\delta^2, \tag{2.10}$$

where $v''(\ell_0)$ is the second derivative of v with respect to ℓ evaluated at $\ell = \ell_0$, $V \equiv v''(\ell_0)\ell_0^2$, and $v'(\ell) = 0$ at $\ell = \ell_0$ [31]. Using (2.9) and (2.10), (2.8) can be written as

$$F_2 \approx \int \mathrm{d}^2\boldsymbol{r}\left[\frac{1}{2}K(\nabla^2\delta)^2 + \frac{1}{2}\Sigma(\nabla\delta)^2 + \frac{1}{2}V\delta^2\right], \tag{2.11}$$

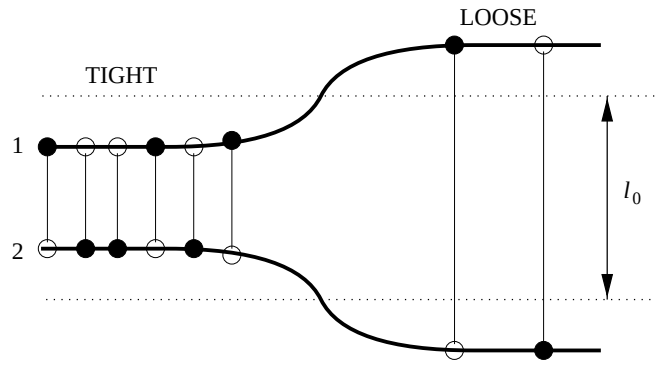

Fig. 4. Schematic representation of two adhering membranes undergoing a lateral phase separation in the case of the bolaform-sticker adhesion. Coexistence between tight (T) and loose (L) membrane domains is shown. The inter-membrane distance is smaller than ℓ_0 for the tight phase, whereas it larger than ℓ_0 for the loose phase.

with $K \equiv \kappa\ell_0^2$ and $\Sigma \equiv \sigma\ell_0^2$. This is the expression of the deformation energy within the harmonic approximation and it served as a starting point to many calculations on membrane adhesion [4,27,29].

Now we will include the effect of the adhesion on the phase separation and suggest a lowest-order coupling between the composition $\phi_i(\boldsymbol{r})$ and the inter-membrane distance $\delta(\boldsymbol{r})$. When the membranes are quenched into a two-phase region of the phase diagram a sticker-poor phase coexists with a sticker-rich phase. As shown in Figure 4, this can lead to different inter-membrane distance for the different membrane domains. Since the sticky segments of the bridges adhere directly onto the two membranes, the coupling is proportional to the sum of the local sticker concentrations of the two membranes. This can be phenomenologically represented by the following coupling term:

$$F_3 = \frac{\alpha}{2\ell_0}\int \mathrm{d}^2\boldsymbol{r}\,(\psi_1+\psi_2)\ell = \alpha\int \mathrm{d}^2\boldsymbol{r}\,\phi_+\delta + \cdots, \quad (2.12)$$

where the coupling constant α is positive preferring smaller separation $\delta < 0$ in regions where the average concentration ϕ_+ is positive (or $\psi_1 + \psi_2 > 2\psi_c$). In the last expression of (2.12), we have neglected the linear terms in ϕ_+ and δ, which merely shift the chemical potential or minimum of the potential, respectively. Depending on the value of ϕ_+, this coupling term not only introduces a shift of the minimum of the potential v but also changes the minimum value of the potential. Note also that (2.12) is symmetric with respect to the exchange of the two membranes $1 \leftrightarrow 2$.

The above linear coupling energy can also be understood in the following way. Let us first consider a single flexible membrane with sticker molecules adhering to a flat substrate. Suppose $v_r(\ell)$ and $v_f(\ell)$ are the potentials for sticker-rich and sticker-free membrane, respectively. Following the same discussion as in (2.10), each of the potential is parabolic around a different separation: $v_r \approx a(\ell-\ell_r)^2$ and $v_f \approx a(\ell-\ell_f)^2$. The effective potential can be obtained by a linear combination of these two potentials, *i.e.*, $(1-\psi)v_f(\ell) + \psi v_r(\ell)$. By expanding $v_f(\ell)$ and $v_r(\ell)$, we get a coupling term which is proportional to $\psi\ell$. In the case of adhesion between two membranes, we add the contributions from both of the membranes and obtain the coupling energy as given in (2.12). The same argument can be repeated for any arbitrary adhesion potentials, $v_f(\ell)$ and $v_r(\ell)$, provided each of them has a single well-defined minimum at some distance ℓ.

The total free energy considered in our model is the sum of (2.4), (2.11), and (2.12):

$$F = F_1 + F_2 + F_3. \quad (2.13)$$

Here it is convenient to convert to Fourier space. The Fourier transform of any function $f(\boldsymbol{r})$ is defined as

$$\tilde{f}(\boldsymbol{q}) = \int \mathrm{d}^2\boldsymbol{r}\, f(\boldsymbol{r})e^{i\boldsymbol{q}\cdot\boldsymbol{r}}, \quad (2.14)$$

where $\boldsymbol{q}$ is the two-dimensional in-plane wave vector. The total free energy can be expressed as

$$\begin{aligned} F = \frac{1}{A}\sum_{\boldsymbol{q}} \Bigg[& \frac{1}{2}(t+cq^2)\big(|\tilde{\phi}_+(\boldsymbol{q})|^2 + |\tilde{\phi}_-(\boldsymbol{q})|^2\big) \\ & + \frac{1}{2}(V+\Sigma q^2 + Kq^4)|\tilde{\delta}(\boldsymbol{q})|^2 + \alpha\tilde{\phi}_+(\boldsymbol{q})\tilde{\delta}(-\boldsymbol{q})\Bigg] \\ & + \int \mathrm{d}^2\boldsymbol{r}\left[\frac{1}{4}(\phi_+^4 + 6\phi_+^2\phi_-^2 + \phi_-^4)\right. \\ & \left. - \mu_+\phi_+ - \mu_-\phi_-\right], \end{aligned} \quad (2.15)$$

where A is the area of the membranes projected on the x-y plane. For convenience the free energy (2.15) is written as a combination of real space and Fourier space terms.

Within the mean-field level, the free energy in terms of ϕ_+ and ϕ_- is obtained by functionally minimizing F with respect to $\tilde{\delta}(\boldsymbol{q})$. Then we find

$$\tilde{\delta}(\boldsymbol{q}) = -\frac{\alpha\tilde{\phi}_+(\boldsymbol{q})}{V+\Sigma q^2 + Kq^4}. \quad (2.16)$$

Hence the inter-membrane distance $\delta = (\ell-\ell_0)/\ell_0$ is fully determined by the value of ϕ_+. By inserting (2.16) into (2.15), the resulting free energy depends only on ϕ_+ and ϕ_-, and becomes

$$\begin{aligned} F = \frac{1}{A}\sum_{\boldsymbol{q}} & \left[\frac{1}{2}\tilde{\Gamma}_+(\boldsymbol{q})|\tilde{\phi}_+(\boldsymbol{q})|^2 + \frac{1}{2}(t+cq^2)|\tilde{\phi}_-(\boldsymbol{q})|^2\right] \\ & + \int \mathrm{d}^2\boldsymbol{r}\left[\frac{1}{4}(\phi_+^4 + 6\phi_+^2\phi_-^2 + \phi_-^4)\right. \\ & \left. - \mu_+\phi_+ - \mu_-\phi_-\right], \end{aligned} \quad (2.17)$$

where

$$\tilde{\Gamma}_+(\boldsymbol{q}) = t + cq^2 - \frac{\alpha^2}{V+\Sigma q^2 + Kq^4}. \quad (2.18)$$

If we expand the last term in (2.18) for small q, we obtain

$$\tilde{\Gamma}_+(\boldsymbol{q}) \approx (t-\gamma) + \left(c + \frac{\alpha^2 \Sigma}{V^2}\right) q^2, \tag{2.19}$$

with

$$\gamma \equiv \frac{\alpha^2}{V}. \tag{2.20}$$

The parameter γ is an important parameter characterizing the coupling strength. The first two terms in (2.19) implies an upward shift of the transition temperature, as will be discussed in detail in the next section. We also find that the presence of the coupling ($\alpha \neq 0$) increases the line tension c provided the mechanical surface tension Σ is non-zero; $c \to c + \alpha^2 \Sigma / V^2$.

3 Phase diagrams

In this section, we calculate the mean-field phase diagrams for bolaform-sticker adhesion using the free energy explained in the previous section. In order to study the bulk properties of the system, we set $\boldsymbol{q} = 0$ and study the homogeneous solutions, ϕ_i's and δ being constants. From (2.16), the inter-membrane distance which minimizes the free energy is given by

$$\delta = -\frac{\alpha \phi_+}{V}. \tag{3.1}$$

Since α is positive, δ is negative (smaller inter-membrane distance) for positive ϕ_+, and δ is positive (larger inter-membrane distance) for negative ϕ_+. By substituting back this δ into the free energy f per unit area for homogeneous (constant) ϕ_+ and ϕ_-, we obtain

$$f = \frac{1}{2}(t-\gamma)\phi_+^2 + \frac{1}{2} t \phi_-^2 + \frac{1}{4}(\phi_+^4 + 6\phi_+^2\phi_-^2 + \phi_-^4) - \mu_+\phi_+ - \mu_-\phi_-, \tag{3.2}$$

where γ is defined in (2.20). Notice that γ is never negative and vanishes only when $\alpha = 0$. Therefore, when $\mu_+ = \mu_- = 0$, the field ϕ_+ will order before ϕ_-, and the phase with $\phi_+ \neq 0$ and $\phi_- = 0$ is expected [32]. Although the phase behavior of this free energy can be examined in general, we concentrate here only on two particular cuts in the parameter space, *i.e.*, $\mu_- = 0$ and $\mu_+ = 0$. In these cases one can clearly see the effect of adhesion on the lateral phase separation.

3.1 The case $\mu_- = 0$

When $\mu_- = 0$ the two membranes have the same chemical potential $\mu_1 = \mu_2$. Since the chemical potential μ_+ is coupled to ϕ_+, f can be minimized first with respect to ϕ_-. A "symmetric phase" is obtained for $t + 3\phi_+^2 > 0$ with

$$\phi_- = 0, \tag{3.3}$$

where the two membranes have the same concentrations, $\phi_1 = \phi_2$. Likewise, two "asymmetric phases" are obtained for $t + 3\phi_+^2 < 0$ with

$$\phi_- = \pm\sqrt{-t - 3\phi_+^2}. \tag{3.4}$$

In the asymmetric phase the two membranes have different concentrations $\phi_1 \neq \phi_2$. After inserting these expressions into (3.2) with $\mu_- = 0$, the free energy becomes

$$f_1 = \begin{cases} \frac{1}{2}(t-\gamma)\phi_+^2 + \frac{1}{4}\phi_+^4 - \mu_+\phi_+, & \text{for } t + 3\phi_+^2 > 0, \\ -\frac{1}{4}t^2 - \frac{1}{2}(2t+\gamma)\phi_+^2 - 2\phi_+^4 - \mu_+\phi_+, & \text{for } t + 3\phi_+^2 < 0. \end{cases} \tag{3.5}$$

Notice that this free energy is continuous at $t = -3\phi_+^2$. This free energy f_1 can now be minimized with respect to ϕ_+. The resulting equation of state is written as

$$\mu_+ = \begin{cases} (t-\gamma)\phi_+ + \phi_+^3, & \text{for } t + 3\phi_+^2 > 0, \\ -(2t+\gamma)\phi_+ - 8\phi_+^3, & \text{for } t + 3\phi_+^2 < 0. \end{cases} \tag{3.6}$$

The phase diagram can now be calculated and the two-phase region is obtained by the Maxwell construction. The phase diagram for $\mu_- = 0$ is illustrated in Figure 5.

For $t > 0$, only the symmetric phase with $\phi_- = 0$ can appear since $t + 3\phi_+^2 > 0$. Two symmetric phases with different ϕ_+ can coexist when $t < \gamma$. The coexistence curve is simply given by

$$\phi_+ = \pm\sqrt{-t+\gamma}, \tag{3.7}$$

and the associated critical point is located at

$$(t, \phi_+, \mu_+)_c = (\gamma, 0, 0). \tag{3.8}$$

We stress that the critical temperature is *increased* from $t_c = 0$ to $t_c = \gamma = \alpha^2/V$ due to the coupling between the composition ϕ_+ and the inter-membrane distance δ as given in (2.12). In other words, the phase separation is *enhanced* by the adhesion of membranes. As presented in Figure 4, the two coexisting values of ϕ_+ given by (3.7) lead to different inter-membrane distances δ according to (3.1). Since $\alpha > 0$, δ is negative ($\ell < \ell_0$) in the sticker-rich domain, and this phase is called the "tight phase" (T). On the other hand, δ is positive ($\ell > \ell_0$) in the sticker-poor domain and this phase is called the "loose phase" (L). However, for each of the coexisting tight and loose phases, $\phi_- = 0$, which means that the sticker concentration is the same in the two membranes, $\phi_1 = \phi_2$.

For $-\gamma/2 < t < 0$, the asymmetric phase with $\phi_- \neq 0$ is always unstable, and the tight and loose phases coexist according to (3.1) and (3.7). For $t < -\gamma/2$, the asymmetric phase can be locally stable but it is only metastable. Namely, its free energy is higher than that of the symmetric phase. Hence the coexistence between the tight and loose phases given by (3.1) and (3.7) preempts the asymmetric phase. The limit of metastability of the asymmetric

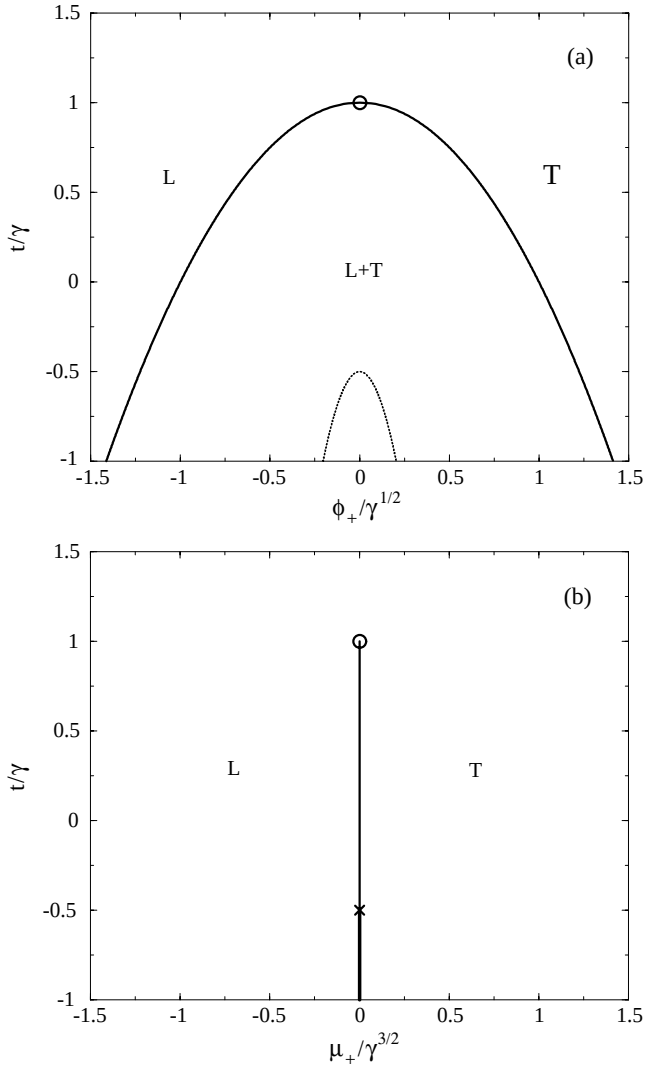

Fig. 5. The phase diagrams for the bolaform-sticker adhesion when $\mu_- = 0$ as a function of (a) rescaled average composition $\phi_+/\gamma^{1/2}$ and temperature t/γ, and (b) rescaled average chemical potential $\mu_+/\gamma^{3/2}$ and temperature t/γ. The continuous line is a first-order phase transition line, whereas the dotted line is the limit of metastability of the asymmetric phase with $\phi_- \neq 0$. The metastable region of the asymmetric phase is indicated by a thick line in (b). Open circle ($\circ$) indicates a critical point. Below the critical temperature, there is a coexistence region between the loose (L) and the tight (T) phases as denoted by L+T. The phase diagram is symmetric with respect to both $\phi_+ \to -\phi_+$ and $\mu_+ \to -\mu_+$.

phase is obtained by calculating the second derivative of the second equation of (3.5) with respect to ϕ_+. This leads to

$$\phi_+ = \pm\sqrt{\frac{-2t-\gamma}{24}}, \tag{3.9}$$

which is also shown as a dotted line inside the L+T coexisting region of Figure 5(a).

In summary, for $\mu_- = 0$, the asymmetric phase $\phi_- \neq 0$ does not exist as a stable phase for any temperature. At most it is metastable and occurs within the L+T coexistence region. The tight and loose phases coexist for $t < \gamma = \alpha^2/V$ according to (3.1) and (3.7).

3.2 The case $\mu_+ = 0$

Next we consider the case of $\mu_+ = 0$ but with $\mu_- \neq 0$. This means that the chemical potentials of the two membranes have the same magnitude but opposite sign, *i.e.*, $\mu_1 = -\mu_2$. This is a special case of the more general situation where the symmetry between the two membranes is explicitly broken. Now f in (3.2) can be minimized with respect to ϕ_+ first. As long as $t + 3\phi_-^2 > \gamma$, the only solution is

$$\phi_+ = 0. \tag{3.10}$$

This is called the "middle phase" (M) where the intermembrane distance is exactly ℓ_0 (or $\delta = 0$). Again note that $\phi_+ = 0$ means that $\psi_1 + \psi_2 = 2\psi_c$. For $t + 3\phi_-^2 < \gamma$, we have the tight (or loose) phase with

$$\phi_+ = \pm\sqrt{-t+\gamma-3\phi_-^2}, \tag{3.11}$$

where ℓ deviates from ℓ_0 (or $\delta \neq 0$) according to (3.1). Since $\mu_+ = 0$, both the tight and the loose phases are energetically degenerated and they coexist. By substituting ϕ_+ back into (3.2) with $\mu_+ = 0$, the free energy becomes

$$f_2 = \begin{cases} \dfrac{1}{2}t\phi_-^2 + \dfrac{1}{4}\phi_-^4 - \mu_-\phi_-\,, \\ \qquad\qquad \text{for} \quad t + 3\phi_-^2 > \gamma\,, \\ -\dfrac{1}{4}(t-\gamma)^2 + \dfrac{1}{2}(-2t+3\gamma)\,\phi_-^2 \\ \quad -2\phi_-^4 - \mu_-\phi_-\,, \\ \qquad\qquad \text{for} \quad t + 3\phi_-^2 < \gamma\,. \end{cases} \tag{3.12}$$

After minimizing with respect to ϕ_-, the equation of state is given as

$$\mu_- = \begin{cases} t\phi_- + \phi_-^3\,, & \text{for} \quad t + 3\phi_-^2 > \gamma\,, \\ (-2t+3\gamma)\,\phi_- - 8\phi_-^3\,, & \text{for} \quad t + 3\phi_-^2 < \gamma\,. \end{cases} \tag{3.13}$$

The calculated phase diagrams for $\mu_+ = 0$ are shown in Figure 6. The phase diagram is symmetric about $\phi_- = 0$ and $\mu_- = 0$ as a consequence of the $\phi_+^2\phi_-^2$ coupling term, and lack of any odd terms in ϕ_+ in the free energy. For $t > \gamma$ there is a one-phase region of the middle phase with $\phi_+ = 0$ since $t + 3\phi_-^2 > \gamma$. For $5\gamma/6 < t < \gamma$, the system undergoes a second-order phase transition between the middle phase ($\phi_+ = 0$) and the tight (or loose) phase ($\phi_+ \neq 0$). The analytical expressions of the second-order phase transition lines are

$$\phi_- = \pm\sqrt{\frac{-t+\gamma}{3}}, \tag{3.14}$$

and

$$\mu_- = \pm\frac{2t+\gamma}{3}\sqrt{\frac{-t+\gamma}{3}}, \tag{3.15}$$

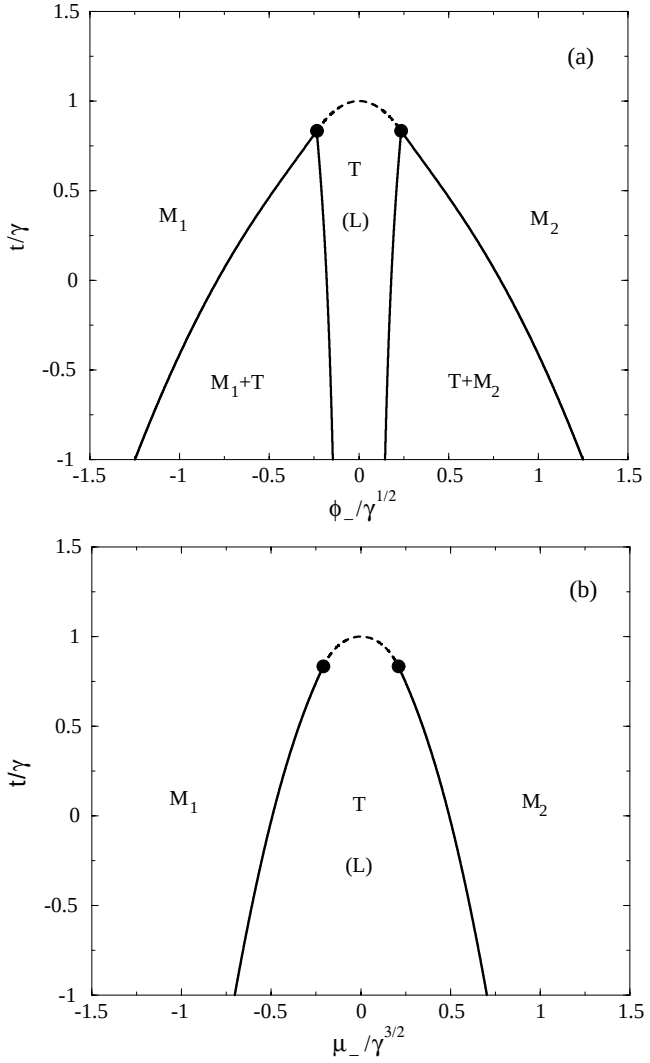

Fig. 6. The phase diagrams for the bolaform-sticker adhesion when $\mu_+ = 0$ as a function of (a) rescaled composition difference $\phi_-/\gamma^{1/2}$ and temperature t/γ, and (b) rescaled chemical potential difference $\mu_-/\gamma^{3/2}$ and temperature t/γ. The continuous line is a first-order phase transition line, whereas the dashed line is a second-order one. The loose, tight and middle phases are denoted as L, T, and M, respectively. The two tricritical points are indicated by a filled circle (•). Below them there are two regions of coexistence of the middle phase ($\phi_+ = 0$) and the tight phase ($\phi_+ \neq 0$) denoted as M_1+T and T+M_2. The phase diagram is symmetric with respect to both $\phi_- \to -\phi_-$ and $\mu \to -\mu_-$. Because $\mu_+ = 0$ there is a degeneracy between the tight (T) and the loose (L) phases on the phase diagram.

in Figure 6, respectively. On the second-order phase transition line, ϕ_+ goes continuously to zero.

For $t < 5\gamma/6$, the transition changes to first order. This has been numerically determined by the Maxwell construction. The point which connects the first- and second-order phase transition lines is a tricritical point [32]. In our model, it is located at

$$(t, \phi_-, \mu_-)_{\rm tcp} = \left(\frac{5}{6}\gamma, \ \pm \frac{1}{3\sqrt{2}}\gamma^{1/2}, \ \pm \frac{4\sqrt{2}}{27}\gamma^{3/2} \right). \tag{3.16}$$

The first-order phase transition corresponds to the coexistence of the middle phase with $\phi_+ = 0$ and the tight (or loose) phase with $\phi_+ \neq 0$. The obtained two-phase coexistence region is indicated by "M+T" in Figure 6(a). Within the present Ginzburg-Landau expansion, the tight phase persists even if we go to low temperatures. Because of the degeneracy between tight and loose phases, the first-order line near the tricritical point actually corresponds to coexistence of three phases: tight, loose, and middle phases.

In continuation to the discussion of the previous subsection ($\mu_- = 0$), we see that the phase separation is also *enhanced* for the $\mu_+ = 0$ parameter space. It occurs at higher temperatures, since the tricritical temperature $t_{\rm tcp} = 5\gamma/6 = 5\alpha^2/6V$ is positive for $\alpha \neq 0$. It is important to notice that in the middle phase with $\phi_+ = 0$, the inter-membrane distance is ℓ_0 since $\delta = 0$. On the other hand, in the tight (loose) phase with $\phi_+ > 0$ ($\phi_+ < 0$), according to (3.1) and (3.7), $\ell < \ell_0$ ($\ell > \ell_0$). The coexisting membrane domains between tight and middle phases, or between loose and middle phases is schematically represented in Figure 7.

We end this section by commenting on the general case when both μ_+ and μ_- are non-zero. When μ_+ becomes non-zero, the degeneracy between the tight and the loose phases is lifted. In such a case, instead of the three-phase coexistence for $\mu_+ = 0$, there is a coexistence between either tight and middle phases, or between loose and middle phases as shown in Figure 7(a) and (b), respectively. Notice that the tricritical point exists only when $\mu_+ = 0$. In a more general phase diagram drawn in the (t, μ_+, μ_-) space, three second-order lines meet at the tricritical point. In the three-dimensional parameter space, these second-order lines lie on the perimeter of two-phase coexistence planes between either tight and middle phases (T+M) or between loose and middle phases (L+M).

4 Non-monotonous membrane profile

One of our assumptions was that the inter-membranes potential $v(\ell; \phi_+ = 0)$ has a single minimum at $\ell = \ell_0$ when $\phi_+ = 0$. In the absence of thermal fluctuations, two homogeneous membranes are bound with inter-membrane distance ℓ_0 for $\phi_+ = 0$. In this section, we calculate the profile of the inter-membrane distance between two membranes which are quenched below the phase separation temperature.

We first expand the potential $v(\ell; \phi_+ = 0)$ up to the fourth-order terms in δ;

$$v(\ell; \phi_+ = 0) \approx v(\ell_0) + \frac{1}{2}V\delta^2 + \frac{1}{4}U\delta^4, \tag{4.1}$$

where $V \equiv v''(\ell_0)\ell_0^2$ as before and $U \equiv v^{(4)}(\ell_0)\ell_0^4 > 0$.

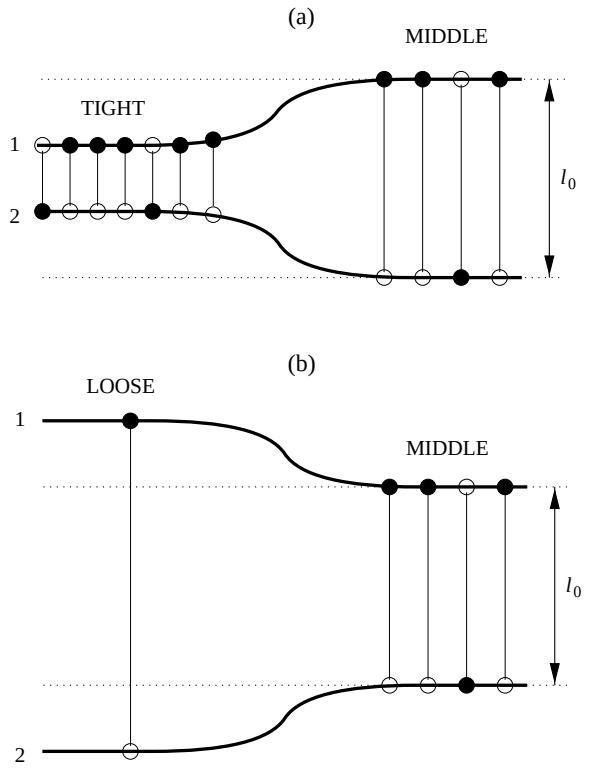

Fig. 7. Schematic drawing of the inter-membrane distance of two adhering membranes with coexisting domains between: (a) tight (T) and middle (M) phases, and; (b) loose (L) and middle (M) phases, as applies from Figure 6 for bolaform-sticker adhesion. The inter-membrane distance is exactly ℓ_0 for the middle phase, whereas it is smaller (larger) than ℓ_0 for the tight (loose) phase.

Both V and U are positive constants because of the convexity of v at its minimum. Suppose that each of the membranes is in its high-temperature phase ($t > 0$). Then the fourth-order ϕ_i terms in the Ginzburg-Landau expansion (2.4) can be neglected since the second-order terms are positive. The resulting free energy with $\mu_+ = \mu_- = 0$ is

$$\begin{aligned} F = \int \mathrm{d}^2\boldsymbol{r} \Big[& \frac{1}{2}c\left[(\nabla\phi_+)^2 + (\nabla\phi_-)^2\right] \\ & + \frac{1}{2}t(\phi_+^2 + \phi_-^2) + \alpha\phi_+\delta \\ & + \frac{1}{2}K(\nabla^2\delta)^2 + \frac{1}{2}\Sigma(\nabla\delta)^2 + \frac{1}{2}V\delta^2 + \frac{1}{4}U\delta^4 \Big] \\ = \frac{1}{A}\sum_{\boldsymbol{q}} \Big[& \frac{1}{2}(t + cq^2)\big(|\tilde\phi_+(\boldsymbol{q})|^2 + |\tilde\phi_-(\boldsymbol{q})|^2\big) \\ & + \alpha\tilde\phi_+(\boldsymbol{q})\tilde\delta(-\boldsymbol{q}) \\ & + \frac{1}{2}(V + \Sigma q^2 + Kq^4)|\tilde\delta(\boldsymbol{q})|^2 \Big] + \int \mathrm{d}^2\boldsymbol{r}\,\frac{1}{4}U\delta^4. \end{aligned} \quad (4.2)$$

We now minimize F with respect to the concentrations $\tilde\phi_+(\boldsymbol{q})$ and $\tilde\phi_-(\boldsymbol{q})$ and obtain

$$\tilde\phi_+(\boldsymbol{q}) = -\frac{\alpha}{t + cq^2}\tilde\delta(\boldsymbol{q}), \qquad \tilde\phi_-(\boldsymbol{q}) = 0. \quad (4.3)$$

By inserting these equations into (4.2) and expanding for small q, the free energy can be written as

$$F = \int \mathrm{d}^2\boldsymbol{r} \left[\frac{1}{2}K_\mathrm{e}(\nabla^2\delta)^2 + \frac{1}{2}\Sigma_\mathrm{e}(\nabla\delta)^2 + \frac{1}{2}V_\mathrm{e}\delta^2 + \frac{1}{4}U_\mathrm{e}\delta^4\right], \quad (4.4)$$

with

$$\begin{aligned} K_\mathrm{e} &\equiv K - \frac{\alpha^2 c^2}{t^3}, \qquad & \Sigma_\mathrm{e} &\equiv \Sigma + \frac{\alpha^2 c}{t^2}, \\ V_\mathrm{e} &\equiv V - \frac{\alpha^2}{t}, \qquad & U_\mathrm{e} &\equiv U. \end{aligned} \quad (4.5)$$

We see that for $t > 0$ the coupling always increases the mechanical tension $\Sigma_\mathrm{e} > \Sigma$, but reduces the rigidity $K_\mathrm{e} < K$ and the potential strength $V_\mathrm{e} < V$.

Let us consider the strong coupling case when $V_\mathrm{e} < 0$ but still having $K_\mathrm{e} > 0$, namely,

$$V < \frac{\alpha^2}{t} < K\left(\frac{t}{c}\right)^2. \quad (4.6)$$

For $t > 0$, although no phase separation occurs in the absence of coupling ($\alpha = 0$), it occurs for non-zero α. The minimum free energy of the membranes is given by solving the Euler-Lagrange equation obtained by minimizing (4.4) with respect to the inter-membrane distance δ:

$$K_\mathrm{e}\nabla^4\delta - \Sigma_\mathrm{e}\nabla^2\delta + V_\mathrm{e}\delta + U_\mathrm{e}\delta^3 = 0. \quad (4.7)$$

The two uniform (bulk) solutions of (4.7) are

$$\delta_0 = \pm\sqrt{-V_\mathrm{e}/U_\mathrm{e}}. \quad (4.8)$$

We assume a one-dimensional profile $\delta(x)$ describing the inter-membrane distance along the x-direction. A typical profile determined by a numerical solution of the Euler-Lagrange equation (4.7) using a relaxational method is shown in Figure 8. It is convenient to rescale the variables δ and x as $\zeta = U_\mathrm{e}^{1/3}\delta$ and $u = K_\mathrm{e}^{-1/4}U_\mathrm{e}^{1/12}x$, respectively, yielding the following one-dimensional profile equation:

$$\frac{\mathrm{d}^4\zeta}{\mathrm{d}u^4} - \left(\frac{\Sigma_\mathrm{e}}{K_\mathrm{e}^{1/2}U_\mathrm{e}^{1/6}}\right)\frac{\mathrm{d}^2\zeta}{\mathrm{d}u^2} + \left(\frac{V_\mathrm{e}}{U_\mathrm{e}^{1/3}}\right)\zeta + \zeta^3 = 0. \quad (4.9)$$

Only two independent combinations of the four parameters K_e Σ_e, V_e and U_e exist. In Figure 8 they are set to be $\Sigma_\mathrm{e}/(K_\mathrm{e}^{1/2}U_\mathrm{e}^{1/6}) = 0.1$ and $V_\mathrm{e}/U_\mathrm{e}^{1/3} = -1$, respectively. The profile has a large slope at the interface $x = u = 0$, but relaxes to the bulk values $\pm\delta_0$ at $x = \pm\infty$ in a non-monotonic fashion with two symmetric overshoots, having a height greater than δ_0. These overshoots are suppressed by increasing Σ_e or by increasing the coupling strength α. The maximum value of δ at the overshoot scales as $|V_\mathrm{e}|^{1/2}$ as can be seen from (4.8). The overshoot of the profile is

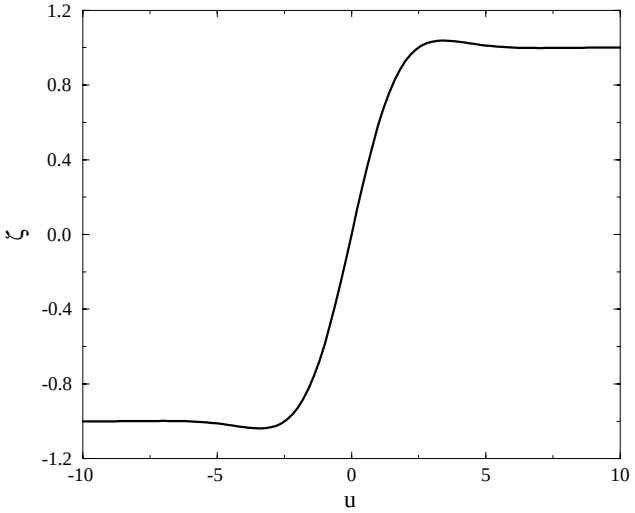

Fig. 8. Inter-membrane distance profile at the domain boundary. The variables are rescaled as $\zeta = U_e^{1/3}\delta$ and $u = K_e^{-1/4}U_e^{1/12}x$. The values of the two independent parameters are chosen to be $\Sigma_e/(K_e^{1/2}U_e^{1/6}) = 0.1$ and $V_e/U_e^{1/3} = -1$.

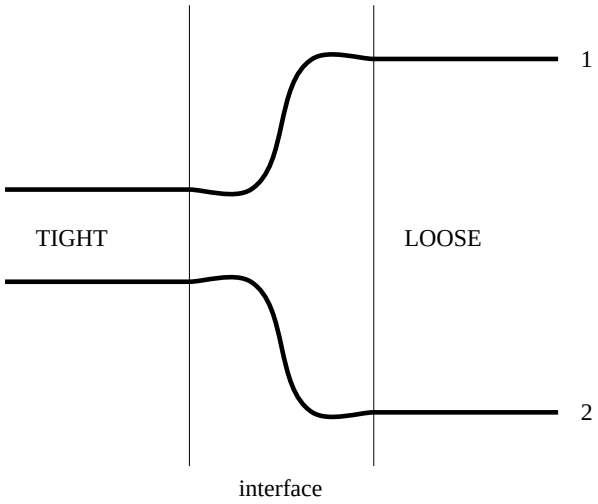

Fig. 9. Schematic drawing of the domain boundary and inter-membrane distance of two adhering membranes. Two symmetric overshoots in the interface region between the loose and tight domains are shown, in agreement with the model and Figure 8. They result from the combined effect of membrane curvature and lateral tension.

followed by a damped oscillation which minimizes the curvature energy. This behavior is similar to the non-linear response of membranes to local pinning sites [33–35] or membranes adhering to a geometrically structured substrate [29] and is a result of the 4th-order derivative in the profile equation. The oscillatory decay has been also predicted for the membrane profile between two inclusions such as proteins [36–39].

The configuration of the phase separated membranes corresponding to the above inter-membrane distance δ is schematically represented in Figure 9. In the case of the adhesion of a single flexible membrane onto a supported membrane, the supported membrane cannot have any shape fluctuations. Therefore, the inter-membrane distance profile calculated in this section can be regarded as a distance of the flexible membrane from the substrate with respect to its equilibrium distance ℓ_0.

5 Discussion

5.1 Main findings

In this paper, the interplay between adhesion and lateral phase separation of multi-component membranes is investigated. We consider the "bolaform-sticker" adhesion where adhesive bridges are formed by a single sticker having two sticky segments and adhere directly onto the two membranes, as shown in Figure 1(a). We proposed a phenomenological free energy consisting of three parts: i) the free energy describing the lateral phase separation of stickers on each membrane (see (2.2)); ii) the deformation energy of the two membranes, which is the sum of the bending energy, the surface tension, and the potential energy (see (2.6)); and, iii) the coupling energy between the inter-membrane distance and the average concentration of stickers on both membranes (see (2.12)). The difference of the chemical potentials between the two membranes is also taken into account because the sticker concentrations do not have to be the same.

We calculate the phase diagrams describing the bulk properties for two particular choices of the chemical potentials, *i.e.*, $\mu_- = 0$ $(\mu_1 = \mu_2)$ and $\mu_+ = 0$ $(\mu_1 = -\mu_2)$. In the case of $\mu_- = 0$, the critical temperature increases depending on the coupling strength and the potential strength (see (3.8)). Hence the lateral phase separation is *enhanced* due to the adhesion. This is one of the main consequences of our model. When the phase separation takes place, the inter-membrane distance is smaller for the domains rich in the sticker molecules ("tight phase"), and larger for the domains poor in the stickers ("loose phase"). In the case of $\mu_+ = 0$, our model exhibits a tricritical behavior. The upward shift of the tricritical temperature also indicates the *enhancement* of the lateral phase separation.

We find that the line tension for the lateral phase separation increases because of the coupling effect as long as the mechanical surface tension is non-zero. We have also calculated the inter-membrane distance profile between the two membranes which are quenched below their phase separation temperature. Because the membrane shape is governed by the bending rigidity, the inter-membrane distance profile relaxes to the bulk values in a non-monotonic way with two symmetric overshoots.

5.2 Membrane adhesion on solid surfaces and supported membranes

So far, we have mainly discussed the adhesion of two membranes. Our model also applies to the case where a single flexible membrane with sticker molecules adheres to a flat

substrate or a supported membrane [20]. Let us discuss these two cases separately. For a flat substrate without any supported membrane on it, the contributions from the second membrane (say $i = 2$) can be dropped from the model. The coupling term (2.12) simply reduces to $\alpha\phi_1\delta$ because the stickers are assumed to adhere directly to the substrate. The second case is that of a supported membrane with sticker molecules. Unlike the case of two fluctuating membranes discussed in Section 4, the supported membrane does not have any shape fluctuations. However, even in such situations, there is an enhancement of the phase separation due to the coupling effect and the upward shift of the critical temperature is given by (3.8). Another related situation is the case where a membrane is composed of two different lipids and the membrane is put close to a flat substrate. If the two lipids feel different hydration force and prefer different distances from the substrate, the phase separation between the two components will be enhanced by the adhesion for the same reason described in this paper.

5.3 Relation to other models

There exists an analogy between the phase behavior of our membrane system with that of metamagnets (magnets which undergo fist-order phase transitions in an increasing magnetic field) or ^{3}He-^{4}He mixtures described by the BEG (Blume-Emery-Griffith) spin-one model [40,41]. Moreover, the phase diagrams for $\mu_+ = 0$ are analogous to those describing the phase separation of two-component mixtures in fluid bilayers which also exhibits tricritical behavior [42] and other related amphiphilic systems [43–47]. However, in the former case of two-component bilayers the concentration difference between the two leaflets of the membrane is linearly coupled to the curvature of the bilayer and the difference in the chemical potential is not taken into account.

In our paper, we did not address the problem of the unbinding transition. We rather assumed that the membranes are always bound together, even in the absence of any sticker molecules. This assumption is partially motivated by the experimental study of reference [23] where suspended membrane (part of the giant vesicle) was claimed to be bound to the supporting membrane even in the absence of sticker molecules. In this case, the inter-membrane distance ℓ stays finite and it is permissible to expand the free energy around the minimum. Hence the phase separation consists of loosely and tightly bound patches. The interplay between unbinding transition and phase separation of multi-component membranes has been considered in other theoretical works [14–16]. The adhesion there is only brought about by sticker molecules, and the phase separation is induced both by attractive interactions and fluctuation-induced interactions between the stickers. Although their model treats a different aspect of the more general problem, the fluctuation effect yields similar consequences compared to ours. We assumed that the *cis*-interaction in (2.2) is attractive, and tracing over the inter-membrane distance δ yields a term proportional to $\gamma\phi_+^2$. Since this term does not depend on the sign of ϕ_+, it has a similar effect as fluctuations although our treatment is restricted to the mean-field level.

It is worthwhile to comment here the difference between the present study and that of reference [23]. In their paper, it is found that the adhesion between the membranes including homophilic recognition molecules and repeller molecules is controlled by lateral phase separation. The multiple competing states of adhesion is attributed to the double-well inter-membrane interaction potential generated by the competition of two forces; attraction between homophilic molecules and the repulsion between repeller molecules. By changing the repeller concentration, the double-minimum potential causes the first-order transition between a state with inter-membrane spacing set by the thickness of the repeller molecules to a state with a spacing set by the bare potential (van der Waals plus hydration interactions). In our work, the effect of repeller molecules is not taken into account and the minimum of the potential depends on the sticker concentration through the coupling term (2.12). When the stickers are phase separated and two different values of the sticker concentration coexist, the inter-membrane potential has double-minimum. However the physical origin of this double-minimum potential is different from that in reference [23] because it is not due to the presence of repeller molecules.

5.4 Other types of sticker molecules

As mentioned in the introduction, "homophilic-sticker" adhesion occurs when the adhesive bridges are formed by two stickers of the same type bound together by their two sticky segments (see Fig. 1(b)). Suppose ψ_i $(i = 1, 2)$ denotes the sticker concentration on each membrane. Then the inter-membrane distance depends on the product of each sticker concentration expressing the probability to have two stickers —one on each membrane— at the same position. Using (2.1) this coupling term can be written in terms of ϕ_i as

$$\psi_1\psi_2 = \phi_1\phi_2 + \psi_c(\phi_1 + \phi_2) + \psi_c^2. \qquad (5.1)$$

An interesting remark can be made for homophilic-sticker adhesion. The resulting phase separation within each membrane leads to three different values for the inter-membrane distance. The inter-membrane distance between domains rich in stickers on both membranes (rich-rich), as well as between rich-poor domains, and poor-poor domains can be different [14,15]. Notice that these three different inter-membrane distances correspond to the tight, middle, and loose phases in our model.

A third case is that of "lock-and-key" adhesion due to the formation of chemical bonds between lock-and-key types of stickers, *e.g.,* ligands and receptors (see Fig. 1(c)). Suppose that both types of stickers are distributed on the two membranes and ψ_i now represents the local concentration, say, of the lock molecules. First let us assume

that the membranes are saturated with sticker molecules (no lipid). Then, $1-\psi_i(\boldsymbol{r})$ represents the concentration of key molecules. Since domains rich in lock (key) molecules on one membrane adhere with domains rich in key (lock) molecules on the other membrane, the coupling term in the free energy F_3 will be a coupling between the inter-membrane distance and

$$\psi_1(1-\psi_2)+(1-\psi_1)\psi_2 = -2\phi_1\phi_2+(1-2\psi_c)(\phi_1+\phi_2)+2\psi_c(1-\psi_c). \quad (5.2)$$

This term is symmetric with respect to the exchange of two membranes. Both in (5.1) and (5.2), we see that the lowest-order term in the concentration (except the constant term) is proportional to ϕ_+. If there is a linear coupling between the inter-membrane distance and ϕ_+ in these cases, we expect an upward shift in the transition temperature and the phase separation will be enhanced as argued above. Due to the presence of higher-order terms in (5.1) and (5.2), however, the phase behavior will be more complex.

Let us now take into account the presence of lipids in the lock-and-key adhesion. If a single type of sticker is present on each membrane, namely, lock molecules on membrane 1 and key molecules on membrane 2, we can regard ψ_1 and ψ_2 as the concentrations of lock and key molecules embedded in the lipid membrane, respectively. Then $1-\psi_1$ and $1-\psi_2$ describe the concentration of the second component (lipid) on each membrane, respectively. In this case, the inter-membrane distance depends on $\psi_1\psi_2$ as in (5.1). When both lock and key molecules are present on both membranes, one has to start with a three-component mixture for each of the membranes. The generic lattice model to study the behavior of ternary membranes of monolayers is the BEG spin-one model [40, 41,48]. Here one has to include the coupling between the two membranes. If we denote the concentration of lock and key molecules on each membrane as ψ_i^{L} and ψ_i^{K} (and hence the concentration of the dilution lipid is $1-\psi_i^{\mathrm{L}}-\psi_i^{\mathrm{K}}$), the inter-membrane distance now depends on $\psi_1^{\mathrm{L}}\psi_2^{\mathrm{K}}+\psi_1^{\mathrm{K}}\psi_2^{\mathrm{L}}$ which is similar to (5.2). More detailed calculations for the homophilic stickers and lock-and-key stickers and their influence on membrane adhesion are left for future studies.

We have greatly benefited from the discussions and correspondence with R. Lipowsky, R. Netz, J. Rädler, E. Sackmann, and T. Weikl. SK would like to thank the Ministry of Education, Science and Culture, Japan for providing financial support during his visit to Israel. Support from the exchange program between the Japan Society for the Promotion of Science (JSPS) and the Israel Ministry of Science and Technology is also gratefully acknowledged. DA acknowledges partial support from the Israel Science Foundation founded by the Israel Academy of Sciences and Humanities, Centers of Excellence Program and the US-Israel Binational Science Foundation (BSF) under grant number 98-00429.

References

1. B. Alberts, D. Bray, J. Lewis, M. Raff, K. Roberts, J.D. Watson, *Molecular Biology of the Cell* (Garland, New York, 1994).
2. E. Sackmann, FEBS Lett. **346**, 3 (1994).
3. R. Lipowsky, S. Leibler, Phys. Rev. Lett. **56**, 2541 (1986).
4. U. Seifert, R. Lipowsky, Phys. Rev. A **42**, 4768 (1990).
5. G.I. Bell, Science **200**, 618 (1978).
6. G.I. Bell, M. Dembo, P. Bongrand, Biophys. J. **45**, 1051 (1984).
7. E.A. Evans, Biophys. J. **48**, 175 (1985); Biophys. J. **48**, 185 (1985).
8. D.E. Leckband, J.N. Israelachvili, F.-J. Schmitt, W. Knoll, Science **255**, 1419 (1992).
9. E.-L. Florin, V.T. Moy, H.E. Gaub, Science **264**, 415 (1994).
10. V.T. Moy, E.-L. Florin, H.E. Gaub, Science **266**, 257 (1994).
11. W. Müller, H. Ringsdorf, E. Rump, G. Wildbug, X. Zhang, L. Angermaier, W. Knoll, M. Liley, J. Spinke, Science **262**, 1706 (1993).
12. D. Zuckerman, R. Bruinsma, Phys. Rev. Lett. **74**, 3900 (1995).
13. D. Zuckerman, R. Bruinsma, Phys. Rev. E **57**, 964 (1998).
14. R. Lipowsky, Phys. Rev. Lett. **77**, 1652 (1996).
15. R. Lipowsky, Colloids Surf. A **128**, 255 (1997).
16. T.R. Weikl, R.R. Netz, R. Lipowsky, Phys. Rev. E. **62**, 45 (2000); T.R. Weikl, R. Lipowsky, to be published in Langmuir (2000).
17. D.A. Noppl-Simson, D. Needham, Biophys. J. **70**, 1391 (1996).
18. A. Albersdörfer, T. Feder, E. Sackmann, Biophys. J. **73**, 245 (1997).
19. A. Albersdörfer, R. Bruinsma, E. Sackmann, Europhys. Lett. **42**, 227 (1998).
20. J.O. Rädler, T.J. Feder, H.H. Strey, E. Sackmann, Phys. Rev. E **51**, 4526 (1995).
21. J. Nardi, T. Feder, R. Bruinsma, E. Sackmann, Europhys. Lett. **37**, 371 (1997).
22. J. Nardi, R. Bruinsma, E. Sackmann, Phys. Rev. E **58**, 5340 (1998).
23. R. Bruinsma, A. Behrisch, E. Sackmann, Phys. Rev. E, **61**, 4253 (2000).
24. S.L. Keller, W.H. Pitcher III, W.H. Huestis, H.M. McConnell, Phys. Rev. Lett. **81**, 5019 (1998).
25. S.L. Keller, H.M. McConnell, Phys. Rev. Lett. **82**, 1602 (1999).
26. S.A. Safran, *Statistical Thermodynamics of Surfaces, Interfaces, and Membranes* (Addison Wesley, New York, 1994).
27. R. Bruinsma, M. Goulian, P. Pincus, Biophys. J. **67**, 746 (1994).
28. The Derjaguin approximation is treated in, *e.g.*, J. Israelachivili, *Intermolecular and Surface Forces* (Academic, San Diego, 1992). Deviations from the Derjaguin approximation in vesicle adhesion problems can be found, *e.g.*, in reference [29].
29. P.S. Swain, D. Andelman, Langmuir **15**, 8902 (1999).
30. If the two membranes have different rigidity, κ_1 and κ_2, the effective rigidity is given by $\kappa=\kappa_1\kappa_2/(\kappa_1+\kappa_2)$. Similar relation holds for the surface tension. See reference [14].

31. When the minimum of the potential is determined only by the balance between hydration and van der Waals interactions (in the absence of any sticker molecules), typical values are given by $\ell_0 \approx 3 \times 10^{-9}$m, $v(\ell_0) \approx -5 \times 10^{-6}$J/m^2, and $V \approx 2 \times 10^{-4}$J/m^2. See reference [29].
32. P.M. Chaikin, T.C. Lubensky, *Principles of Condensed Matter Physics* (Cambridge, New York, 1995).
33. R. Bar-Ziv, R. Menes, E. Moses, S.A. Safran, Phys. Rev. Lett. **75**, 3356 (1995).
34. R. Menes, S.A. Safran, Phys. Rev. E **56**, 1891 (1997).
35. R. Menes, S.A. Safran, D. Kessler, Europhys. Lett. **40**, 225 (1997).
36. N. Dan, P. Pincus, S.A. Safran, Langmuir **9**, 2768 (1993).
37. N. Dan, A. Berman, P. Pincus, S.A. Safran, J. Phys. II **4**, 1713 (1994).
38. H. Aranda-Espinoza, A. Berman, N. Dan, P. Pincus, S.A. Safran, Biophys. J. **71**, 648 (1996).
39. R.R. Netz, J. Phys. II **7**, 833 (1997).
40. M. Blume, V.J. Emery, R.B. Griffiths, Phys. Rev. A **4**, 1071 (1971).
41. J.M. Kincaid, E.G.D. Cohen, Phys. Rep. **22**, 57 (1975).
42. F.C. MacKintosh, S.A. Safran, Phys. Rev. E **50**, 2891 (1994).
43. S. Leibler, D. Andelman, J. Phys. (Paris) **48**, 2013 (1987).
44. H. Kodama, S. Komura, J. Phys. II **3**, 1305 (1993).
45. J.L. Harden, F.C. MacKintosh, Europhys. Lett. **28**, 495 (1994).
46. P.L. Hansen, L. Miao, J.H. Ipsen, Phys. Rev. E **58**, 2311 (1998).
47. S. Villain-Guillot, D. Andelman, Eur. Phys. J. B **4**, 95 (1998).
48. P.B.S. Kumar, G. Gompper, R. Lipowsky, Phys. Rev. E **60**, 4610 (1999).